

RESEARCH ARTICLE

View Article Online

View Journal | View Issue

Cite this: *Inorg. Chem. Front.*, 2023, **10**, 5678Received 9th June 2023,
Accepted 7th August 2023

DOI: 10.1039/d3qi01081c

rsc.li/frontiers-inorganic

Chalcogen atom abstraction from NCE^- ($\text{E} = \text{O}, \text{S}, \text{Se}$) and $\text{i-Pr}_2\text{S}$ by the excited state of a luminescent tricyano osmium(vi) nitride†Li-Xin Wang,^{‡a} Miaomiao Zhou,^{‡b} Lu-Lu Liu,^a Jing Xiang,^{id}*^a Ji-Yan Liu,^a
Kai-Chung Lau^{id}*^b and Tai-Chu Lau^{id}*^b

Upon irradiation by blue LED ($\lambda > 460$ nm), the tricyano osmium nitrido complex $[\text{Os}^{\text{VI}}(\text{N})(\text{L})(\text{CN})_3]^-$ (**OsN**) in its excited state readily abstracts chalcogen atoms from the anions NCE^- ($\text{E} = \text{O}, \text{S}, \text{Se}$) to give the corresponding metal chalcogenonitrosyls $[\text{Os}^{\text{II}}(\text{N}=\text{E})(\text{L})(\text{CN})_3]^-$ (**OsNE**) and CN^- . A similar S atom abstraction also occurs in the photoreaction of **OsN** with organic sulfide, such as diisopropyl sulfide, to give **OsNS** and **Os-N=C(CH₃)₂**. The molecular structures of $(\text{PPh}_4)[\text{Os}^{\text{II}}(\text{N}=\text{E})(\text{L})(\text{CN})_3]$ have been determined by X-ray crystallography, which show N–O, N–S and N–Se bond distances of 1.206, 1.507 and 1.675 Å, respectively.

Introduction

Metal nitrido complexes ($\text{M}=\text{N}$) have been proposed as key intermediates in N_2 fixation; they are also potentially useful reagents for the nitrogenation of various organic substrates.^{1–5} A number of electrophilic nitrido complexes have been reported recently. For instance, *cis*- and *trans*- $[\text{Os}^{\text{VI}}(\text{N})(\text{tpy})\text{Cl}_2]^+$ ($\text{tpy} = 2,2':6',2''$ -terpyridine) have been shown to exhibit novel electrophilic properties. A variety of reagents such as phosphines, amines, cyanide, azide, arylboranes, amine *N*-oxides, alkenes, and benzenethiols have been reported to react with the osmium nitrido complexes.⁶ Higher reactivity is found for $\text{Ru}=\text{N}$ and $\text{Fe}=\text{N}$, such as $[\text{Ru}(\text{N})(\text{salchda})(\text{MeOH})]^+$ ($\text{salchda} = N,N'$ -bis(salicylidene)-*o*-cyclohexyldiamine dianion)⁷ and $[\text{PhB}(\text{RIm})_3\text{Fe}=\text{N}]$ ($\text{Im} = \text{imidazol}$, $\text{R} = \text{'Bu}, \text{Mes}, \text{and } ^1\text{Pr}_2$).⁸ Although these nitrido complexes exhibit novel electrophilic properties and react readily with a variety of nucleophiles, their reactivity is still relatively limited compared to analogous metal-oxo ($\text{M}=\text{O}$) species.⁹

In search of more reactive $\text{M}=\text{N}$ species that are comparable to $\text{M}=\text{O}$, we recently started to investigate the reactivity of

$\text{M}=\text{N}$ in their excited states. Accordingly, a highly luminescent $\text{Os}(\text{vi})$ nitrido complex, $[\text{Os}^{\text{VI}}(\text{N})(\text{L})(\text{CN})_3]^-$ (**OsN**, $\text{HL} = 2$ -(2-hydroxy-5-nitrophenyl)benzoxazole) with long-lived LMCT excited state has been prepared.¹⁰ This species is highly reactive in the excited state (**OsN***) due to its nitridyl $[\text{Os}=\text{N}^*]$ character. Indeed, upon irradiation with visible light ($\lambda > 460$ nm), **OsN*** readily activates the strong C–H bonds of alkanes and arenes,¹¹ undergoes oxidative *N*-dealkylation of various tertiary amines¹² and C–O bond cleavage of dihydroxybenzene,¹³ exhibits formal N atom transfer to aliphatic secondary amines¹⁴ and ring-nitrogenation of aromatic amines.¹⁵ Recently, we have also found that **OsN*** could activate both α - and δ -C–H bonds of alcohols in the presence of PhIO , due to the formation of the highly potent oxidant PhIO^+ ¹⁶ (Fig. 1).

We report herein that **OsN*** readily undergoes unprecedented chalcogen atom abstraction from the stable inorganic anions NCE^- ($\text{N} = \text{O}, \text{S}, \text{Se}$), as well as from organic sulfide such as $\text{i-Pr}_2\text{S}$.

Results and discussion

Upon irradiation of a solution of **OsN** in CH_2Cl_2 containing 10 equiv. of $(\text{PPh}_4)\text{NCSe}$ with blue LED ($\lambda > 460$ nm) for 24 h, the bright yellow solution turned pale-yellow. Electrospray ionization mass spectrometry (ESI/MS, $-ve$ mode) of the resulting solution exhibits a new peak at m/z 617, which is assigned to $[\text{Os}(\text{N}=\text{Se})(\text{L})(\text{CN})_3]^-$ (**OsNSE**). Similarly, ESI/MS for the photoreaction of **OsN** with 10 equiv. of $(\text{PPh}_4)\text{NCS}$ for 48 h shows a major peak at m/z 571, which is assigned to $[\text{Os}(\text{N}=\text{S})(\text{L})(\text{CN})_3]^-$ (**OsNS**) (Fig. 2 and S1†). When the reactions were

^aKey Laboratory of Optoelectronic Chemical Materials and Devices (Ministry of Education), School of Optoelectronic Materials and Technology, Jiangnan University, Wuhan, 430056, China. E-mail: xiangjing@yangtzeu.edu.cn

^bDepartment of Chemistry, City University of Hong Kong, Tat Chee Avenue, Kowloon Tong, Hong Kong, China. E-mail: bhtclau@cityu.edu.hk

†Electronic supplementary information (ESI) available: Experimental section, crystal data, ESI/MS, and ^1H NMR. CCDC 2267408–2267410. For ESI and crystallographic data in CIF or other electronic format see DOI: <https://doi.org/10.1039/d3qi01081c>

‡These two authors contributed equally.



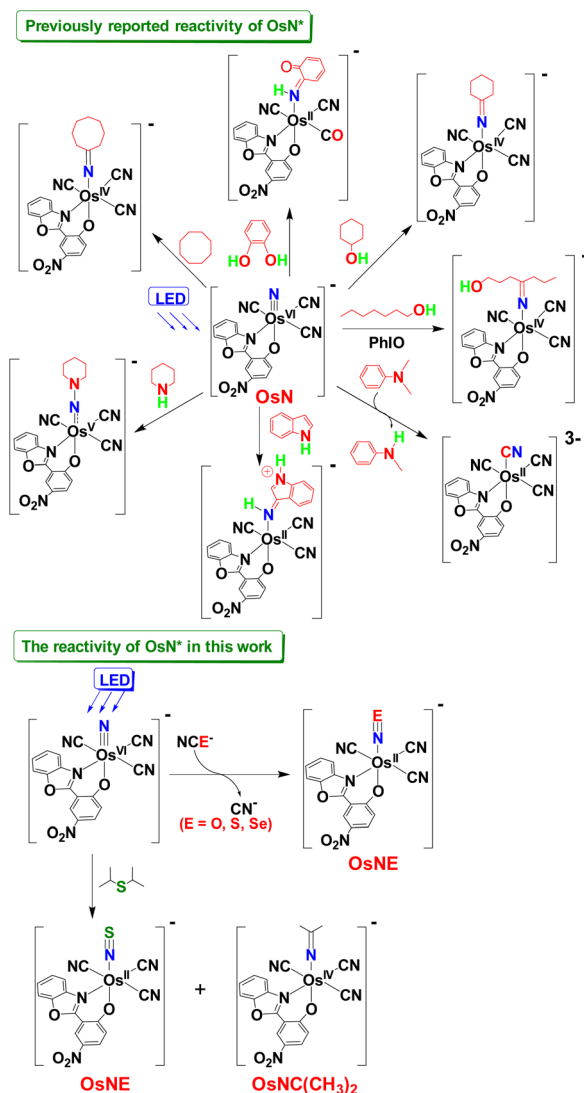


Fig. 1 (a) Reported reactivity of OsN^* towards various substrates; (b) reaction of OsN^* with NCE^- and $i\text{-Pr}_2\text{S}$ in this work.

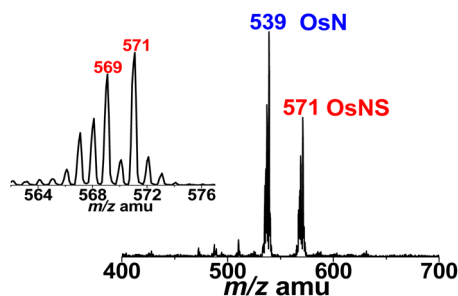


Fig. 2 ESI/MS of the photoreaction of OsN with 10 equiv. of $(\text{PPh}_4)\text{NCS}$ for 24 h showing a new product peak at m/z 571 (OsNS).

carried out on a preparative scale, $(\text{PPh}_4)[\text{Os}(\text{N}=\text{E})(\text{L})(\text{CN})_3]$ (OsNE , $\text{E} = \text{Se}$ and S) were isolated as light yellow crystalline solids with 45% and 52% yields, respectively. ESI/MS (–ve

mode) of these photoreaction solutions also show a small peak at $m/z = 26$ due to the formation of CN^- . M-NE complexes have been prepared from the reaction of metal nitrides with S_8 or elemental Se .^{17–19} However, to the best of our knowledge, S/Se atom transfer from NCE^- anions, which involves cleavage of strong $\text{C}=\text{E}$ bonds, has not been reported. The photoreaction of OsN with $(\text{PPh}_4)\text{NCO}$ has also been investigated; however, its reaction rate is much slower, and the yield of $(\text{PPh}_4)[\text{Os}(\text{N}=\text{O})(\text{L})(\text{CN})_3]$ (OsNO)^{20,21} is only $\sim 10\%$, which is probably due to the stronger $\text{C}=\text{O}$ bond than $\text{C}=\text{S}$ and $\text{C}=\text{Se}$ bonds in NCE^- . O atom transfer to metal nitride usually occurs with oxidants such as Me_3NO .^{17a} When ^{15}N -labelled Os^{15}N was used, ESI/MS shows that the parent OsNE ions all increases by one mass unit, indicating that the N atoms in OsNE are from the nitrido ligand rather than from NCE^- .

Both OsNS and OsNSE are stable for >2 weeks in the solid state or in various solvents at room temperature. However, upon exposure to air for more than two months, these complexes were partially converted into OsNO (m/z 555). Attempts were also made to synthesize the tellurium analog (OsNTe) from the photoreaction of OsN and NCTe^- . However, no products could be isolated, presumably due to the instability of the $[\text{Os}(\text{N}=\text{Te})(\text{L})(\text{CN})_3]^-$ species. Also, no reaction of OsN^* with elemental tellurium in various solvents was observed, presumably due to the poor solubility of Te .

The IR spectrum of OsNSE shows strong $\nu(\text{C}=\text{N})$ stretches at 2148, 2133 cm^{-1} and $\nu(\text{N}=\text{Se})$ stretch at 1136 cm^{-1} . Similar $\nu(\text{C}=\text{N})$ stretches in OsNS and OsNO are also found at 2149, 2133 cm^{-1} and 2150, 2139 cm^{-1} , respectively; while the $\nu(\text{N}=\text{S})$ and $\nu(\text{N}=\text{O})$ stretches occur at 1291 cm^{-1} and 1849 cm^{-1} , respectively. The ratio of $\nu(\text{N}=\text{O})$ to $\nu(\text{N}=\text{S})$ stretching frequencies in OsNO and OsNS is 1.432, a typical value for structurally similar NO and NS compounds.²² The UV/vis spectra of these compounds show strong absorption bands due to ligand centered $\pi\text{-}\pi^*$ transitions below 400 nm, with molar extinction coefficients (ϵ) on the order of $10^4 \text{ M}^{-1} \text{ cm}^{-1}$ (Fig. 3a). OsNO also shows a weak absorption band tailing down to the visible region, while for OsNS and OsNSE there is a well-defined absorption band in the visible region; these are tentatively assigned to the O^-N ligand to metal (Os) charge transfer (LMCT) (Fig. S2 and S3†). All compounds are diamagnetic, as evidenced by their sharp proton signals in the normal range in their ^1H NMR spectra (Fig. S4–S6†).

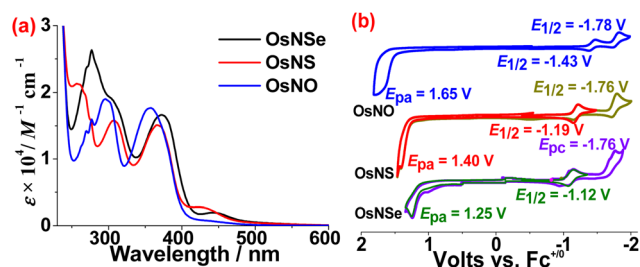


Fig. 3 (a) UV/vis spectra of OsNE in CH_3CN ; (b) CV of OsNE in CH_3CN containing 0.1 M $[\text{tBu}_4\text{N}](\text{PF}_6)$ with a scan rate of 0.1 V s^{-1} .



Cyclic voltammetry (CV) of **OsNE** was conducted in 0.1 M [ⁿBu₄N](PF₆) CH₃CN solution. As shown in Fig. 3b, these compounds all show two reduction waves. The first reduction potentials $E_{1/2}$ are in the range of −1.12 to −1.43 V (vs. Fc^{+/0}), which are dependent on the coordinated NE⁺ ligand with the order of NSe (−1.12 V) > NS (−1.19 V) > NO (−1.43 V). Thus, the first reduction waves are tentatively assigned to the ligand-centered NE^{+/0} reduction. On the other hand, the second reduction waves have very similar potentials for these complexes, hence they are assigned to the reduction of the O[−]N ligand. **OsNE** also exhibits an irreversible wave with E_{pa} of **OsNO** (1.65 V) > **OsNS** (1.40 V) > **OsNSe** (1.25 V), in line with the decreasing π -accepting ability of these chalcogenonitrosyl ligands on going from O to Se. Thus, these oxidation waves should be metal centered, since the Os^{II} center is more stabilized by the stronger π -accepting NO ligand.

Molecular structures

The molecular structures of **OsNE** have been determined by X-ray crystallography and selected bond parameters are listed in Table 1. As shown in Fig. 4, the coordination geometries of the metal centers are similar to that of **OsN**. The Os centers are all 6-coordinated by three CN[−] in a meridional configuration, a bidentate O[−]N ligand and a chalcogenonitrosyl ligand. The Os–N4 bond length in the complexes are similar; 1.727(5) Å in **OsNO**, 1.767(5) Å in **OsNS** and 1.749(3) Å in **OsNSe**, indicating that they have double bond character. These bond lengths follow the order: Os–NO < Os–NSe < Os–NS. This trend is also found in the iridium chalcogenonitrosyl series [Ir(NE){N(CHCHP^tBu₂)₂}] [PF₆].²³ The Os1–N4–E bonds are close to linear; 174.1(4)°, 177.8(4)°, 175.4(2)°, respectively, for E = O, S, Se. The N–E bond lengths are 1.206(6) Å, 1.507(5) Å, and 1.675(3) Å, respectively, for E = O, S, Se, which are very close to the sum of the covalent radii of the double bonds; N–O = 1.17 Å; N–S = 1.54 Å; N–Se = 1.67 Å. The Os–O1_(phenoxy) bond lengths are comparable to the value of 2.024(2) Å in (PPh₄)[Os(NH₃)(L)(CN)₃],¹³ indicating the absence of the strong *trans* influence for these chalcogenonitrosyl ligands.

In our previous work, we showed that **OsN**^{*} readily undergoes an initial one-electron oxidation of various substrates,^{12–16} hence it is reasonable to propose that the present photoreactions proceed *via* an initial 1e[−] transfer (ET) from NCE[−] to **OsN**^{*} to generate **Os^VN** and the NCE[•] radical;

Table 1 Selected bond parameters (Å, °) for **OsNE**

	OsNO	OsNS	OsNSe
Os1–N4	1.727(5)	1.767(5)	1.749(3)
Os1–C2	2.082(7)	2.084(8)	2.069(4)
Os1–C3	2.041(5)	2.037(6)	2.020(4)
Os1–C1	2.091(7)	2.083(8)	2.066(4)
Os1–N5	2.129(4)	2.117(5)	2.127(3)
Os1–O1	2.022(3)	2.034(4)	2.037(2)
N4–E	1.206(6)	1.507(5)	1.675(3)
Os1–N4–E	174.1(4)	177.8(4)	175.4(2)
O1–Os1–N4	174.4(2)	177.1(2)	175.3(1)

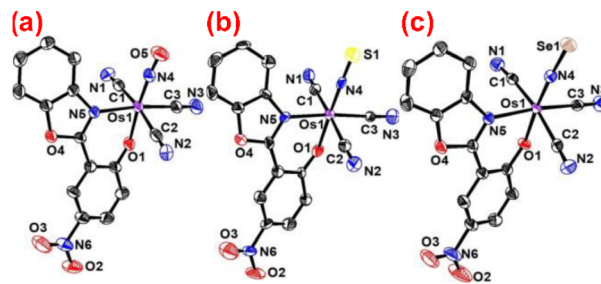


Fig. 4 The structures of the anions **OsNO** (a), **OsNS** (b), and **OsNSe** (c).

this is followed by rapid recombination of the two species to afford the unstable intermediate [Os^{IV}(L)(CN)₃(N–ECN)]^{2−}, which then undergoes spontaneous E–CN bond cleavage to produce **OsNE** and CN[−] (Fig. 5). The estimated reduction potentials (E°) for NCE[•]/NCE[−] are 1.27 V, 1.63 V, and 2.15 V for E = Se, S, and O, respectively.²⁴ The observed reaction rates are inversely dependent on the E° values, consistent with ET being involved in the rate-determining step.

Reaction of **OsN**^{*} with diisopropyl sulfide

The above results indicate that **OsN**^{*} readily abstracts various chalcogen atoms from NCE[−]. A similar reaction occurs between **OsN**^{*} and organic sulphide such as diisopropyl sulfide (i-Pr₂S). Upon irradiation of a solution of **OsN** with 300 equiv. of i-Pr₂S in CH₂Cl₂ for 4 h, ESI/MS shows two new product peaks at *m/z* 571 and 581 (Fig. 6), which are assigned to **OsNS** and [Os^{IV}(L)(CN)₃(N=C(CH₃)₂)][−] (**Os–N=C(CH₃)₂**),¹² respectively (Fig. 7). The reaction was also followed by UV/vis spectroscopy, which shows that the absorption band due to **OsN** gradually decreases, while those of the products gradually increase with time (Fig. S7†). When the reaction was carried out on a preparative scale, the two species were isolated with a molar ratio of ~1 : 2.

Oxidative desulfurization is an important process for the removal of sulfur from liquid fuels. In this process, sulfur-containing compounds are converted to their corresponding sulfones/sulfoxides using various oxidants.²⁵ To the best of our knowledge, direct S atom abstraction from S-containing substrates has yet to be reported. The proposed mechanism for the reaction of **OsN**^{*} with i-Pr₂S is shown in Fig. 8. The first step is ET from i-Pr₂S to **OsN**^{*} to produce **Os^VN** and the radical cation i-Pr₂S^{•+}, this is followed by their combination to give the Os(IV) species (**I**). **I** then undergoes an internal 2e[−] transfer to give an Os(II) species (**II**). This is followed by rapid oxidation of

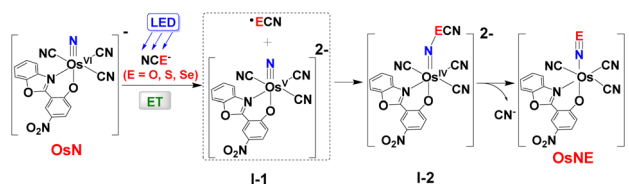


Fig. 5 Proposed mechanism for the reaction of **OsN**^{*} with NCE[−].



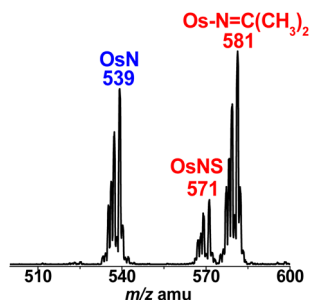


Fig. 6 ESI/MS of the photoreaction of OsN with excess *i*-Pr₂S for 24 h.

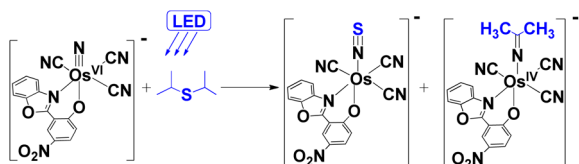


Fig. 7 The photoreaction of OsN with *i*-Pr₂S.

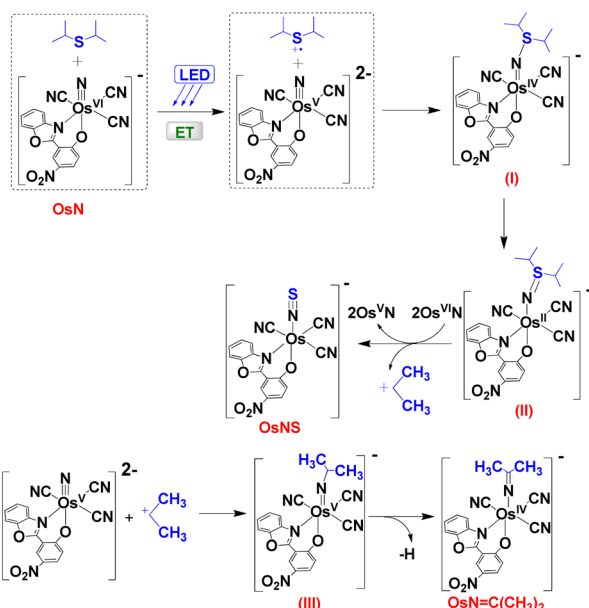


Fig. 8 Proposed mechanism for the reaction of OsN* with *i*-Pr₂S.

II by two 2OsN*, resulting C–S bond cleavage and the formation of Os^VN, OsNS, and CH₃CH⁺CH₃. CH₃CH⁺CH₃ then adds to the nitrido ligand of Os^VN to form the Os(v) species III, which further undergoes an internal 1e[−] oxidative dehydrogenation to afford Os–N=C(CH₃)₂.¹²

We have carried out DFT calculations on the reaction of OsN* + NCS[−] and OsN* + *i*-Pr₂S (Fig. S9† and Fig. 9), which support our proposed mechanisms. As shown in Fig. 9, the reaction is downhill in energy after the initial combination of Os^VN and the radical cation *i*-Pr₂S^{•+} to give the Os(IV) species. The Os(IV) species then undergoes an internal 2e[−] transfer to

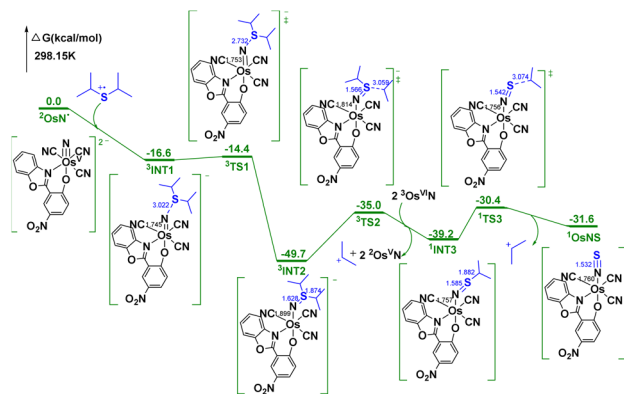


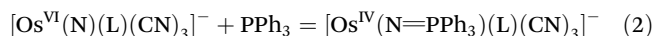
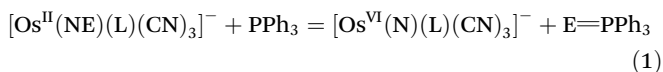
Fig. 9 Gibbs free energy profile for reaction of OsN* with *i*-Pr₂S at the B3LYP-D3(BJ)/def2-TZVPD level.

give an Os(II) species (³INT2) and this is followed by rapid oxidation of ³INT2 by two 2Os^VN, resulting in C–S bond cleavage and the formation of Os^VN, OsNS, and CH₃CH⁺CH₃.

Dechalcogenation of OsNE

Dechalcogenation of OsNS and OsNSE occur readily by using PPh₃. As shown in Fig. 10a, ESI/MS of OsNS with 100 equiv. of PPh₃ for 6 h at 313 K shows a new product peak at *m/z* 801, which is tentatively assigned to [Os^{IV}(L)(CN)₃(N=PPh₃)][−] (Os^{IV}N=PPh₃).²⁶ A minor peak also occurs at *m/z* 539, which is due to OsN, suggesting that OsN may be an intermediate that further reacts with excess PPh₃ to give Os^{IV}N=PPh₃. The reaction rate of OsNSE with PPh₃ is much faster; as shown in Fig. 10b, the ESI/MS for the reaction of OsNSE with 5 equiv. of PPh₃ for 0.5 h at 298 K shows two major product peaks at *m/z* 539 and 801, while the parent peak at *m/z* 617 disappears completely.

The reaction of OsNE (E = S, Se) with PPh₃ can be represented by the following equation.



When the reactions were carried out on a preparative scale, SPPH₃ and SePPH₃ were formed and could be extracted with

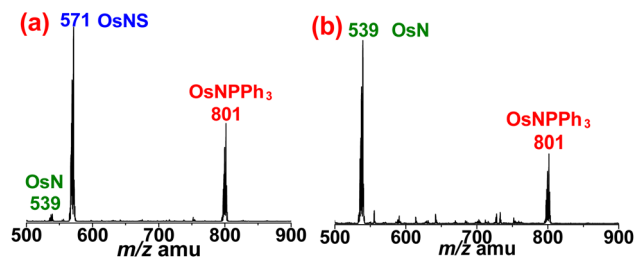


Fig. 10 (a) ESI/MS for OsNS with 100 equiv. of PPh₃ in CH₂Cl₂ at 313 K for 6 h; (b) ESI/MS for OsNSE with 5 equiv. of PPh₃ in CH₂Cl₂ at 298 K for 0.5 h.



Et₂O with >80% yield (Fig. 11). Although for both **OsNS** and **OsNSe**, the Os(IV) phosphineiminato complex [Os^{IV}(L)(CN)₃(N=PPh₃)][−] (**Os^{IV}N=PPh₃**, *m/z* 801) could be observed by ESI/MS, the osmium product that was actually isolated (after chromatography) is the osmium(III) complex [Os^{III}(L)(CN)₃(NH=PPh₃)][−] with PPh₄⁺ counter ion in ~70% yield (**Os^{III}NH=PPh₃**). ESI/MS (−ve mode) of **Os^{III}NH=PPh₃** in MeOH shows a predominant parent anion peak at *m/z* 802, which is one mass unit higher than **Os^{IV}N=PPh₃**. Presumably **Os^{IV}N=PPh₃** is reduced to **Os^{III}NH=PPh₃** during the work-up. The IR spectrum of **Os^{III}NH=PPh₃** shows ν(C≡N) stretches at 2113 and 2084 cm^{−1}, and ν(N–H) stretches at 3276 cm^{−1}. It has a room-temperature magnetic moment of 1.91μ_B (Gouy method, solid sample), consistent with its formulation as a low-spin d⁵ Os^{III} compound. The CV of **Os^{III}NH=PPh₃** in CH₃CN containing 0.1 M [ⁿBu₄N](PF₆) shows a quasi-reversible Os(III/II) couple at *E*_{1/2} = −1.27 V (vs. Fc^{+/0}) (Fig. S8†). There is also a broad wave at ~0.17 V, which is tentatively assigned to **Os^{IV}N=PPh₃**/**Os^{III}NH=PPh₃**.

Oxidative dechalcogenation of **OsNSe** and **OsNS** also occurs by using PhIO (Fig. 12), which is much more rapid than with PPh₃. Upon mixing **OsNS** or **OsNSe** with 5 equiv. of PhIO for 0.5 h in CH₃CN, ESI/MS (−ve mode) for both solutions show a predominant peak at *m/z* 539. When the reactions were carried out on a preparative scale, **OsN** could be isolated with >90% yield, indicating that **OsNSe** and **OsNS** were almost quantitatively converted to **OsN** by PhIO. Moreover, ESI/MS (−ve mode) for the **OsNS** + PhIO solution also shows a minor peak at *m/z* 81, possibly due to HSO₃[−]. On the other hand, for the reaction of **OsNSe** with PhIO, a grey precipitate was observed, which is presumably SeO₂. However, no reaction of **OsNO** with PhIO was observed, probably due to its much stronger N–O bond.

Conclusions

We have demonstrated that **OsN*** readily undergoes unprecedented chalcogen atom abstraction from NCE[−] and i-Pr₂S; such reaction has not been observed even by metal oxo species. We propose that these reactions occur by initial one-electron oxidation of the substrates by **OsN***. The resulting **OsNE** products readily undergoes dechalcogenation by using PPh₃ or PhIO. Notably PhIO regenerates **OsN** from **OsNE**, which suggests that it is possible to construct a catalytic cycle for dechalcogenation of substrates based on OsN/PhIO/visible light.

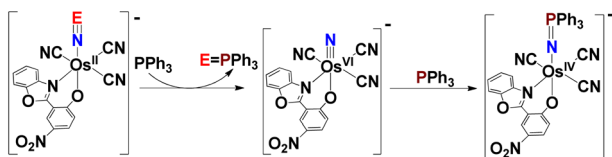


Fig. 11 Chalcogen abstraction by PPh₃ from **OsNE** (E = S, Se).

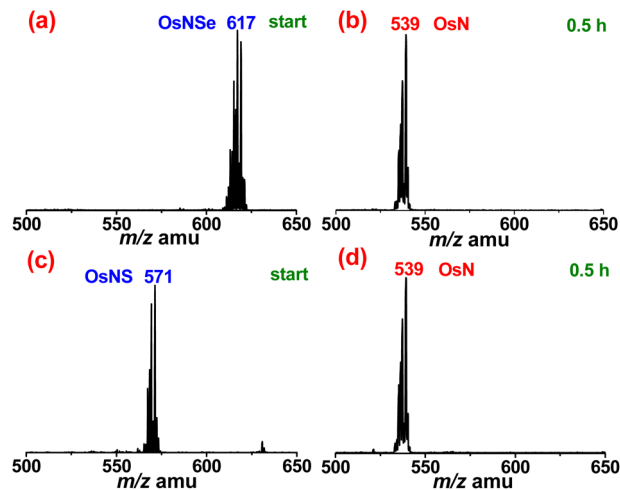


Fig. 12 (a) ESI/MS of **OsNSe** and (b) after addition of 5 equiv. PhIO for 0.5 h in CH₃CN; (c) ESI/MS of **OsNS** and (d) after addition of 5 equiv. PhIO for 0.5 h in CH₃CN.

Experimental

(PPh₄)[Os(NSe)(L)(CN)₃] (**OsNSe**)

Ten Pyrex tubes (15 × 2 cm) each containing **OsN** (5 mg, 5.7 μmol) and (PPh₄)NCSe (12 mg, 27 μmol) in CH₂Cl₂ were irradiated with blue LED light (λ > 460 nm) for 96 h, whereby the light-yellow solutions became pale yellow. The solvent was removed by a rotary evaporator and the residue was dissolved in a minimum amount of CH₂Cl₂ and then loaded onto a silica gel column. The pale yellow band was eluted by CH₂Cl₂/acetone (v:v, 5:1). (PPh₄)[Os(NSe)(L)(CN)₃] was obtained as a yellow microcrystalline solid. Yield: 25 mg, 45%. Light yellow crystals were obtained from the slow diffusion of diethyl ether into a CH₂Cl₂ solution of **OsNSe**. Selected IR (KBr disc, cm^{−1}): ν(C≡N) 2148 and 2133; ν(N=Se) 1136; ESI/MS (−ve mode): *m/z* 617 ([M][−]); UV/vis (CH₃CN): λ_{max} [nm] (ε [mol^{−1} dm³ cm^{−1}]): 256 (21 320), 277sh (15 950), 307 (15 770), 367 (15 080), 427sh (2750). ¹H NMR (400 MHz, CDCl₃): δ 8.89 (d, *J* = 2.9 Hz, 1H, Ar-H), 8.29–8.23 (m, 1H, Ar-H), 7.95–7.89 (m, 5H, Ar-H and PPh₄-H), 7.80 (td, *J* = 7.8, 3.6 Hz, 8H, PPh₄-H), 7.75–7.71 (m, 1H, Ar-H), 7.70–7.62 (m, 8H, PPh₄-H), 7.53 (dt, *J* = 10.9, 3.7 Hz, 2H, Ar-H), 6.52 (d, *J* = 9.3 Hz, 1H, Ar-H). Calcd (%) for C₄₀H₂₇N₆O₄OsPSe: C, 50.26; H, 2.85; N, 8.79; found: C, 50.28; H, 2.81; N, 8.76.

(PPh₄)[Os(NS)(L)(CN)₃] (**OsNS**)

The synthesis of **OsNS** is similar to that of **OsNSe** except (PPh₄)NCS (23 mg, 58 μmol) was used instead. Yield for **OsNS**: 27 mg, 52%. Selected IR Selected IR (KBr disc, cm^{−1}): ν(C≡N) 2149 and 2133; ν(N=S) 1291; ESI/MS (−ve mode): *m/z* 571 ([M][−]); UV/vis (CH₃CN): λ_{max} [nm] (ε [mol^{−1} dm³ cm^{−1}]): 270sh (23 710), 277 (26 320), 302sh (19 240), 374 (16 600), 447 (1940). ¹H NMR (400 MHz, CDCl₃): δ 8.90 (d, *J* = 2.9 Hz, 1H, Ar-H), 8.15–8.11 (m, 1H, Ar-H), 7.95–7.89 (m, 5H, Ar-H and PPh₄-H), 7.80 (td, *J* = 7.8, 3.6 Hz, 8H, PPh₄-H), 7.75–7.70 (m, 1H, Ar-H),



7.70–7.62 (m, 8H, PPh₄-H), 7.56–7.49 (m, 2H, Ar-H), 6.51 (d, *J* = 9.3 Hz, 1H, Ar-H). Calcd (%) for C₄₀H₂₇N₆O₄OsPS: C, 52.86; H, 2.99; N, 9.25; found: C, 52.82; H, 3.02; N, 9.27.

(PPh₄)[Os(NO)(L)(CN)₃] (OsNO)

The synthesis of **OsNO** is similar to that of **OsNSe** except (PPh₄)NCO (22 mg, 58 μmol) was used instead. Yield for **OsNO**: 5 mg, 10%. The **OsNO** also could be obtained from oxidation of the guanidine precursor (**OsG**) by excess *m*-chloroperbenzoic acid (*m*-cpba) in CH₃CN with about 60% yield.^{20,21} Selected IR (KBr disc, cm⁻¹): ν(C≡N) 2150 and 2139; ν(N≡O) 1849; ESI/MS (–ve mode): *m/z* 555 ([M][–]); UV/vis (CH₃CN): λ_{max} [nm] (ε [mol⁻¹ dm³ cm⁻¹]): 270 (14 210), 277 (15 950), 295 (18 980), 357 (17 660), 435sh (760). ¹H NMR (400 MHz, CDCl₃): δ 8.92 (s, 1H, Ar-H), 8.03 (d, *J* = 9.5 Hz, 1H, Ar-H), 7.92 (t, *J* = 7.4 Hz, 4H, PPh₄-H), 7.80 (d, *J* = 7.8 Hz, 8H, PPh₄-H), 7.73 (t, *J* = 7.4 Hz, 2H, Ar-H), 7.65 (dd, *J* = 12.8, 7.9 Hz, 8H, PPh₄-H), 7.58–7.50 (m, 2H, Ar-H), 6.70 (d, *J* = 9.3 Hz, 1H, Ar-H). Calcd (%) for C₄₀H₂₇N₆O₅OsP: C, 53.81; H, 3.05; N, 9.41; found: C, 53.76; H, 3.02; N, 9.44.

Dechalcogenation of OsNE

(PPh₄)[Os^{III}(L)(CN)₃(NH=PPh₃)] (**OsNH=PPh₃**). **OsNSe** (20 mg, 20.8 μmol) and PPh₃ (55 mg, 0.2 mmol) were dissolved in CH₂Cl₂ and stirred at room temperature for 6 h to give a dark red solution. The solvent was removed by a rotary evaporator and the residue was dissolved in a minimum amount of CH₂Cl₂ and then loaded onto a silica gel column. The red band was eluted by CH₂Cl₂/MeOH (v:v, 10:1). **OsNH=PPh₃** was isolated as a red microcrystalline solid. Yield: 16.7 mg, 70%. Selected IR (KBr disc, cm⁻¹): ν(C≡N) 2113 and 2084; ν(N-H) 3276; ESI/MS (–ve mode): *m/z* 802 ([M][–]); μ_{eff} = 1.91 μ_B; UV/vis (CH₃CN): λ_{max} [nm] (ε [mol⁻¹ dm³ cm⁻¹]): 263sh (15 180), 268(15 790), 275(15 760), 290sh (14 800), 311(14 790), 392 (12 810), 440sh (10 580), 550sh (970). Calcd (%) for C₅₈H₄₃N₆O₄OsP₂: C, 61.10; H, 3.80; N, 7.37; found: C, 61.13; H, 3.78; N, 7.39.

Author contributions

The manuscript was written through the contributions of all authors. All authors have given approval to the final version of the manuscript.

Conflicts of interest

There are no conflicts to declare.

Acknowledgements

This work was supported by the National Natural Science Foundation of China (21771026), the Excellent Discipline Cultivation Project by JHUN (2023XKZ038), the Natural Science Foundation of Jingzhou Science and Technology Bureau

(2022CC54-05) and “Laboratory for Synthetic Chemistry and Chemical Biology” under the Health@InnoHK Program launched by Innovation and Technology Commission, The Government of Hong Kong Special Administrative Region of the People’s Republic of China. KCL and TCL also acknowledge financial support from a NSFC_RGC Joint Research Scheme (N_CityU111/20).

References

- 1 R. A. Eikey and M. M. Abu-Omar, Nitrido and Imido Transition Metal Complexes of Groups 6–8, *Coord. Chem. Rev.*, 2003, **243**, 83–124.
- 2 J. F. Berry, Terminal Nitrido and Imido Complexes of the Late Transition Metals., *Comments Inorg. Chem.*, 2009, **30**, 28–66.
- 3 S. J. K. Forrest, B. Schluschaß, E. Y. Yuzik-Klimova and S. Schneider, Nitrogen Fixation via Splitting into Nitrido Complexes, *Chem. Rev.*, 2021, **121**, 6522–6587.
- 4 J. M. Smith, Reactive Transition Metal Nitride Complexes, *Prog. Inorg. Chem.*, 2014, **58**, 417–470.
- 5 (a) M. N. Cosio and D. C. Powers, Prospects and challenges for nitrogen-atom transfer catalysis, *Nat. Rev. Chem.*, 2023, **7**, 424–438; (b) T. Itabashi, K. Arashiba, A. Egi, H. Tanaka, K. Sugiyama, S. Sugimoto, S. Kuriyama, K. Yoshizawa and Y. Nishibayashi, Direct synthesis of cyanate anion from dinitrogen catalysed by molybdenum complexes bearing pincer-type ligand, *Nat. Commun.*, 2022, **13**, 6161; (c) M. Fritz, S. Rupp, C. I. Kiene, S. Kisan, J. Telser, C. Würtele, V. Krewald and S. Schneider, Photoelectrochemical Conversion of Dinitrogen to Benzonitrile: Selectivity Control by Electrophile- versus Proton-Coupled Electron Transfer, *Angew. Chem., Int. Ed.*, 2022, **61**, e202205922; (d) J. Song, Q. Liao, X. Hong, L. Jin and N. Mézailles, Conversion of Dinitrogen into Nitrile: Cross-Metathesis of N₂-Derived Molybdenum Nitride with Alkynes, *Angew. Chem., Int. Ed.*, 2021, **60**, 12242–12247.
- 6 (a) T. J. Meyer and M. H. V. Huynh, The Remarkable Reactivity of High Oxidation State Ruthenium and Osmium Polypyridyl Complexes, *Inorg. Chem.*, 2003, **42**, 8140–8160; (b) A. G. Maestri, K. S. Cherry, J. J. Toboni and S. N. Brown, [4+1] Cycloadditions of Cyclohexadienes with Osmium Nitrides, *J. Am. Chem. Soc.*, 2001, **123**, 7459–7460; (c) M. H. V. Huynh, T. J. Meyer, M. A. Hiskey and D. L. Jameson, Os(II)–Nitrosyl and Os(II)–Dinitrogen Complexes from Reactions between Os(VI)–Nitrido and Hydroxylamines and Methoxylamines, *J. Am. Chem. Soc.*, 2004, **126**, 3608–3615; (d) P. Q. Kelly, A. S. Filatov and M. D. Levin, A Synthetic Cycle for Heteroarene Synthesis by Nitride Insertion, *Angew. Chem., Int. Ed.*, 2022, **61**, e202213041; (e) H.-X. Wang, L. Wu, B. Zheng, L. Du, W.-P. To, C.-H. Ko, D. L. Phillips and C.-M. Che, C–H Activation by an Iron-Nitrido Bis-Pocket Porphyrin Species, *Angew. Chem., Int. Ed.*, 2021, **60**, 4796–4803; (f) D. Martelino, S. Mahato, W. VandeVen, N. M. Hein,



- R. M. Clarke, G. A. MacNeil, F. Thomas and T. Storr, Chromium Nitride Umpolung Tuned by the Locus of Oxidation, *J. Am. Chem. Soc.*, 2022, **144**, 11594–11607; (g) H. Shi, H. K. Lee, Y. Pan, K.-C. Lau, S.-M. Yiu, W. W. Y. Lam, W.-L. Man and T.-C. Lau, Structure and Reactivity of a Manganese(vi) Nitrido Complex Bearing a Tetraamido Macrocyclic Ligand, *J. Am. Chem. Soc.*, 2021, **143**, 15863–15872.
- 7 (a) W.-L. Man, W. W. Y. Lam and T.-C. Lau, Reactivity of Nitrido Complexes of Ruthenium(vi), Osmium(vi), and Manganese(v) Bearing Schiff Base and Simple Anionic Ligands, *Acc. Chem. Res.*, 2014, **47**, 427–439, and ref therein. (b) W.-L. Man, J. Xie, P.-K. Lo, W. W. Y. Lam, S.-M. Yiu, K.-C. Lau and T.-C. Lau, Functionalization of Alkynes by a (Salen)ruthenium(vi) Nitrido Complex, *Angew. Chem., Int. Ed.*, 2014, **53**, 8463–8466; (c) J. Xie, W.-L. Man, C.-Y. Wong, X. Chang, C.-M. Che and T.-C. Lau, Four-Electron Oxidation of Phenols to p-Benzoquinone Imines by a (Salen)ruthenium(vi) Nitrido Complex, *J. Am. Chem. Soc.*, 2016, **138**, 5817–5820.
 - 8 (a) S. B. Muñoz III, W.-T. Lee, D. A. Dickie, J. J. Scepaniak, D. Subedi, M. Pink, M. D. Johnson and J. M. Smith, Styrene Aziridination by Iron(iv) Nitrides, *Angew. Chem., Int. Ed.*, 2015, **54**, 10600–10603; (b) J. L. Martinez, H.-J. Lin, W.-T. Lee, M. Pink, C.-H. Chen, X. Gao, D. A. Dickie and J. M. Smith, Cyanide Ligand Assembly by Carbon Atom Transfer to an Iron Nitride, *J. Am. Chem. Soc.*, 2017, **139**, 14037–14040; (c) D. W. Crandell, S. B. Muñoz, J. M. Smith and M.-H. Baik, Mechanistic study of styrene aziridination by iron(iv) nitrides, *Chem. Sci.*, 2018, **9**, 8542–8552; (d) G. E. Cutsail III, B. W. Stein, D. Subedi, J. M. Smith, M. L. Kirk and B. M. Hoffman, EPR, ENDOR, and Electronic Structure Studies of the Jahn–Teller Distortion in an Fe^v Nitride, *J. Am. Chem. Soc.*, 2014, **136**, 12323–12336; (e) J. J. Scepaniak, C. S. Vogel, M. M. Khusniyarov, F. W. Heinemann, K. Meyer and J. M. Smith, Synthesis, Structure, and Reactivity of an Iron(v) Nitride, *Science*, 2011, **331**, 1049–1052; (f) J. J. Scepaniak, R. P. Bontchev, D. L. Johnson and J. M. Smith, Snapshots of Complete Nitrogen Atom Transfer from an Iron(iv) Nitrido Complex, *Angew. Chem., Int. Ed.*, 2011, **50**, 6630–6633; (g) J. J. Scepaniak, M. D. Fulton, R. P. Bontchev, E. N. Duesler, M. L. Kirk and J. M. Smith, Structural and Spectroscopic Characterization of an Electrophilic Iron Nitrido Complex, *J. Am. Chem. Soc.*, 2008, **130**, 10515–10517.
 - 9 (a) B. Meunier, S. P. de Visser and S. Shaik, Mechanism of Oxidation Reactions Catalyzed by Cytochrome P450 Enzymes, *Chem. Rev.*, 2004, **104**, 3947–3980; (b) I. G. Denisov, T. M. Makris, S. G. Sligar and I. Schlichting, Structure and Chemistry of Cytochrome P450, *Chem. Rev.*, 2005, **105**, 2253–2278; (c) S. Fosshat, S. D. M. Siddharatchi, C. L. Baumberger, V. R. Ortiz, F. R. Fronczek and M. B. Chambers, Light-Initiated C–H Activation via Net Hydrogen Atom Transfer to a Molybdenum(vi) Dioxo, *J. Am. Chem. Soc.*, 2022, **144**, 20472–20483; (d) Y. Cao, J. A. Valdez-Moreira, S. Hay, J. M. Smith and S. P. de Visser, Reactivity Differences of Trigonal Pyramidal Nonheme Iron(iv)-Oxo and Iron(iii)-Oxo Complexes: Experiment and Theory, *Chem. – Eur. J.*, 2023, **29**, e202300271; (e) J. A. Valdez-Moreira, D. M. Beagan, H. Yang, J. Telser, B. M. Hoffman, M. Pink, V. Carta and J. M. Smith, Hydrocarbon Oxidation by an Exposed, Multiply Bonded Iron(iii) Oxo Complex, *ACS Cent. Sci.*, 2021, **7**, 1751–1755.
 - 10 L. J. Luo, Q. Q. Su, S. C. Cheng, J. Xiang, W. L. Man, W. M. Shu, M. H. Zeng, S. M. Yiu, C. C. Ko and T. C. Lau, Tunable Luminescent Properties of Tricyanoosmium Nitrido Complexes Bearing a Chelating O[−]N Ligand, *Inorg. Chem.*, 2020, **59**, 4406–4413.
 - 11 J. Xiang, X.-X. Jin, Q.-Q. Su, S.-C. Cheng, C.-C. Ko, W.-L. Man, M. Xue, L. Wu, C.-M. Che and T.-C. Lau, Photochemical Nitrogenation of Alkanes and Arenes by a Strongly Luminescent Osmium(vi) Nitrido complex, *Commun. Chem.*, 2019, **2**, 40.
 - 12 J. Xiang, M. Peng, Y. Pan, L. J. Luo, S. C. Cheng, X. X. Jin, S. M. Yiu, W. L. Man, C. C. Ko, K. C. Lau and T. C. Lau, Visible Light-Induced Oxidative N-dealkylation of Alkylamines by a Luminescent Osmium(vi) Nitrido Complex, *Chem. Sci.*, 2021, **12**, 14494–14498.
 - 13 J. Xiang, J. Zhu, M. Zhou, L. L. Liu, L. X. Wang, M. Peng, B. S. Hou, S. M. Yiu, W. P. To, C. M. Che, K. C. Lau and T. C. Lau, Oxidative C–O bond Cleavage of Dihydroxybenzenes and Conversion of Coordinated Cyanide to Carbon Monoxide Using a Luminescent Os(vi) Cyanonitrido Complex, *Chem. Commun.*, 2022, **58**, 7988–7991.
 - 14 Q. Q. Su, K. Fan, X. D. Huang, J. Xiang, S. C. Cheng, C. C. Ko, L. M. Zheng, M. Kurmoo and T. C. Lau, Field-induced Slow Magnetic Relaxation in Low-spin S=1/2 Mononuclear Osmium(v) Complexes, *Dalton Trans.*, 2020, **49**, 4084–4092.
 - 15 L.-L. Liu, L.-X. Wang, M. Peng, J. Xiang, H. Yang, S.-M. Yiu and T.-C. Lau, Ring Nitrogenation of Aromatic Amines by the Excited State of an Osmium(vi) Nitrido Complex, *Inorg. Chem.*, 2023, **62**, 1447–1454.
 - 16 J. Xiang, Y. Pan, L.-L. Liu, L.-X. Wang, H. Yang, S.-C. Cheng, S.-M. Yiu, C.-F. Leung, C.-C. Ko, K.-C. Lau and T.-C. Lau, Visible Light-Induced Oxidation of Alcohols by a Luminescent Osmium(vi) Nitrido Complex: Evidence for the Generation of PhIO⁺ as a Highly Active Oxidant in the Presence of PhIO, *J. Am. Chem. Soc.*, 2023, **145**, 9129–9135.
 - 17 (a) T. J. Crevier, S. Lovell and J. M. Mayer, Chalcogen Atom Transfer to a Metal Nitrido. The First Transition Metal Selenonitrosyl Complex, *J. Am. Chem. Soc.*, 1998, **120**, 6607–6608; (b) B. L. Tran, R. Thompson, S. Ghosh, X. Gao, C. H. Chen, M. H. Baik and D. J. Mindiola, A Four-Coordinate Thionitrosyl Complex of Vanadium, *Chem. Commun.*, 2013, **49**, 2768–2770.
 - 18 (a) M. G. Scheibel, I. Klopsch, H. Wolf, P. Stollberg, D. Stalke and S. Schneider, Thionitrosyl- and Selenonitrosyliridium Complexes, *Eur. J. Inorg. Chem.*, 2017, **2017**, 1751–1755.



- 2013, **2013**, 3836–3839; (b) H. Y. Ng, W. M. Cheung, E. K. Huang, K. L. Wong, H. H.-Y. Sung, I. D. Williams and W. H. Leung, Ruthenium Chalcogenonitrosyl and Bridged Nitrido Complexes Containing Chelating Sulfur and Oxygen Ligands, *Dalton Trans.*, 2015, **44**, 18459–18468; (c) H. Y. Ng, N. M. Lam, M. Yang, X. Y. Yi, I. D. Williams and W. H. Leung, Ruthenium(VI) Nitrido Complexes with a Sterically Bulky Bidentate Schiff Base Ligand, *Inorg. Chim. Acta*, 2013, **394**, 171–175.
- 19 (a) A. Wu, A. Dehestani, E. Saganic, T. J. Crevier, W. Kaminsky, D. E. Cohen and J. M. Mayer, Reactions of Tp–Os Nitrido Complexes with the Nucleophiles Hydroxide and Thiosulfate, *Inorg. Chim. Acta*, 2006, **359**, 2842–2849; (b) B. W. S. Kolthammer and P. Legzdins, Preparation of Dicarbonyl (eta-5-cyclopentadienyl) Thionitrosylchromium (I). The First Organometallic Thionitrosyl Complex, *J. Am. Chem. Soc.*, 1978, **100**, 2247–2248.
- 20 (a) J. Xiang, W. L. Man, S. M. Yiu, S. M. Peng and T. C. Lau, Reaction of an Osmium(VI) Nitrido Complex with Cyanide: Formation and Reactivity of an Osmium(III) Hydrogen Cyanamide Complex, *Chem. – Eur. J.*, 2011, **17**, 13044–13051; (b) J. Xiang, Q. Wang, S. M. Yiu, W. L. Man, H. K. Kwong and T. C. Lau, Aerobic Oxidation of an Osmium(III) N-Hydroxyguanidine Complex to Give Nitric Oxide, *Inorg. Chem.*, 2016, **55**, 5056–5061.
- 21 (a) J. Xiang, Q. Wang, S. M. Yiu and T. C. Lau, Dual Pathways in the Oxidation of an Osmium(III) Guanidine Complex. Formation of Osmium(VI) Nitrido and Osmium Nitrosyl Complex, *Inorg. Chem.*, 2017, **56**, 2022–2028; (b) J. Xiang, Q.-Q. Su, L.-J. Luo and T.-C. Lau, Synthesis and reactivity of an osmium(III) aminoguanidine complex, *Dalton Trans.*, 2019, **48**, 11404–11410.
- 22 (a) J. W. Dethlefsen, E. D. Hedegård, R. D. Rimmer, P. C. Ford and A. Døssing, Flash and Continuous Photolysis Studies of the Thionitrosyl Complex $\text{Cr}(\text{CH}_3\text{CN})_5(\text{N S})_2^+$ and the Nitric Oxide Analogs: Reactions of Nitrogen Monosulfide in Solution, *Inorg. Chem.*, 2009, **48**, 231–238; (b) J. R. Dethlefsen, A. Døssing and E. D. Hedegård, Electron Paramagnetic Resonance Studies of Nitrosyl and Thionitrosyl and Density Functional Theory Studies of Nitrido, Nitrosyl, Thionitrosyl, and Selenonitrosyl Complexes of Chromium, *Inorg. Chem.*, 2010, **49**, 8769–8778.
- 23 M. G. Scheibel, B. Askevold, F. W. Heinemann, E. J. Reijerse, B. de Bruin and S. Schneider, Closed-shell and Open-shell Square-planar Iridium Nitrido Complexes, *Nat. Chem.*, 2012, **4**, 552–558.
- 24 D. M. Stanbury, Reduction potentials involving inorganic free radicals in aqueous solution, *Adv. Inorg. Chem.*, 1989, **33**, 69–138.
- 25 F. Boshagh, M. Rahmani, K. Rostami and M. Yousefifar, Key Factors Affecting the Development of Oxidative Desulfurization of Liquid Fuels: A Critical Review, *Energy Fuels*, 2022, **36**, 98–132.
- 26 T.-W. Wong, T.-C. Lau and W.-T. Wong, Osmium(VI) Nitrido and Osmium(IV) Phosphoraniminato Complexes Containing Schiff Base ligands, *Inorg. Chem.*, 1999, **38**, 6181–6186.

